Impact of Channel Aging on Massive MIMO Vehicular Networks in Non-isotropic Scattering Scenarios

N.B. When citing this work, cite the original published paper.

(article starts on next page)

Impact of Channel Aging on Massive MIMO Vehicular Networks in Non-isotropic Scattering Scenarios

Huafu Li*, Liqin Ding†, Yang Wang‡, Peng Wu‡ and Zhenyong Wang*
* School of Electronics and Information Engineering, Harbin Institute of Technology, Harbin, China
† Department of Electrical Engineering, Chalmers University of Technology, Gothenburg, Sweden
‡ School of Electronics and Information Engineering, Harbin Institute of Technology, Shenzhen, China
Email: {fairme, yangw}@hit.edu.cn

Abstract—**Massive multiple-input multiple-output (MIMO) relies on accurate channel estimation for precoding and receiving to achieve its claimed performance advantages. When serving vehicular users, the rapid channel aging effect greatly hinders its advantages, and a careful system design is required to ensure an efficient use of wireless resources. In this paper, we investigate this problem for the first time in a non-isotropic scattering scenario. The von Mises distribution is adopted for the angle of arrival (AoA), resulting in a tunable channel temporal correlation coefficient (TCC) model, which can adapt to different AoA spread conditions through the κ parameter and incorporates the isotropic Jakes-Clarke model as a special case. The simulated results in a Manhattan grid-type multi-cell network clearly demonstrate the impact of channel aging on the uplink spectral efficiency (SE) performance and moreover, in order to maximize the area average SE, the size of the transmission block should be optimally selected according to some linear equations of κ.**

I. INTRODUCTION

Offering high spectral efficiency (SE) and superior robustness to multipath fading channels, massive multiple-input multiple-output (MIMO) technology is expected to play a central role in future cellular systems. The advantages of massive MIMO rely significantly on the availability of accurate channel state information (CSI) at the base stations (BSs) for precoding and/or combining a large number of signals across the antenna array. Most of the existing massive MIMO literature adopts the block-fading channel model, which assumes that the channel remains unchanged during the data transmission phase in between two sequential channel trainings [1], [2]. This is a reasonable approximation when the users have limited mobility. However, most data transmission for the low-mobility personal users occurs indoors, while on the other hand, data-hungry machine type communications, in particular, vehicular communications, are emerging [3]–[5]. Due to the high-speed movement of the vehicular users (VUEs), the impact of channel aging on the actual performance of a massive MIMO system becomes consequential.

Channel aging refers to the mismatch between the channel coefficients during the channel estimation and data transmission phases [6]. Since the BSs only have outdated channel estimation for precoding and combining, performance degradation is inevitable. As an example, it has been observed that in a typical industrial scenario, a 4 milliseconds delay in CSI will cause users with moderate mobility (30 km/h) to degrade performance by up to 50% as compared to users with low mobility (3 km/h), even if the number of BS antennas is not that large (32 and 64) [7]. It is therefore of crucial importance to understand the impact of channel aging on massive MIMO in a highly dynamic vehicular communication environment and gain insights that can help improving network design.

We notice that some existing studies have considered the impact of channel aging on the performance of massive MIMO systems [6], [8]–[12]. In all these works, however, the Jakes-Clarke model and the equal Doppler shift assumption are adopted for simplicity. The Jakes-Clarke model assumes an isotropic scattering environment in which the multipath components arrive from all directions with the same probability. With these assumptions, the temporal correlation coefficient (TCC) of the channel is given by the zeroth-order Bessel function of the first kind [6]. In practical scenarios, however, multipath components usually come from a limited angle of arrival (AoA) range and are often concentrated in one direction [13, Example 7.1]. This has been observed by measurements for BS with elevated antennas in a wide range of scenarios [14], [15] and also for mobile devices [16], especially in the street canyon environment [17, Sect. 7.4]. To the best of our knowledge, the impact of channel aging on massive MIMO in such a more realistic non-isotropic scattering environment has not yet been studied. In this paper, we present our preliminary results on this issue.

The von Mises distribution is adopted for the probability density function (PDF) of AoA, which leads to a new channel TCC model and allows us to study the effect of channel aging under different AoA spread conditions by turning a κ parameter. We derive an expression for the uplink (UL) SE that is achievable in a multi-cell massive MIMO system with pilot contamination. The minimum mean-squared error (MMSE) combining vector is also given for the aging channel. In the Manhattan grid scenario, the impact of channel aging on the area mean SE performance is studied under different AoA spread and VUE velocity conditions. The analysis reveals that the transmission block size has to be carefully selected

to maximize the SE performance of the system. In particular, the simulated results have shown that the optimal block size choice is roughly given by a linear equation of κ, whose parameters depend on the adopted combining strategy and VUEs' velocity. Moreover, the isotropic Jakes-Clarke TCC model leads to overly pessimistic performance predictions and wrong guidance for the optimal transmission block design, which will lead to additional channel training costs.

Notations: We use lowercase italic letters, boldface lowercase letters, boldface uppercase letters, and calligraphic letters to represent scalars, column vectors, matrices, and sets, respectively. $(\cdot)^*$, $(\cdot)^{\mathrm{H}}$, $(\cdot)^\dagger$, and $\|\cdot\|$ denote the conjugate, conjugate transpose, pseudo-inverse, and Euclidean norm, respectively. $|\cdot|$ returns the absolute value of a scalar variable and $\mathbb{E}\{\cdot\}$ is the expectation operation. $\mathcal{N}_\mathbb{C}(\mathbf{0},\mathbf{R})$ stands for the multivariate circularly symmetric complex Gaussian distribution with correlation matrix $\mathbf{R}$, and $\mathbf{I}_m$ is the $m \times m$ identity matrix.

II. SYSTEM MODEL

We consider a multi-cell massive MIMO network composed of L BSs, represented by the set $\mathcal{L}$, and operates according to a synchronous time-division duplex (TDD) protocol. Each BS is equipped with M antennas. K single-antenna VUEs, represented by the set $\mathcal{K}$, transmit in UL on a shared frequency subcarrier. Therefore, the channels considered in this work are frequency-flat. Each VUE is associated with a serving BS following certain rules, e.g., based on the received signal strength, while a BS serves multiple VUEs. Time is divided into transmission blocks. The first T symbols in a block are used for UL pilot sequence transmission for channel training, and the subsequent D symbols are used for data transmission.

A. Aging Channel Modeling

The spatially correlated Rayleigh fading channel between VUE k and BS l is denoted using $\mathbf{h}_{kl} \in \mathbb{C}^M$ and is modeled as

$$\mathbf{h}_{kl} \sim \mathcal{N}_\mathbb{C}(\mathbf{0}, \beta_{kl}\mathbf{R}_{kl}), \quad k \in \mathcal{K}, l \in \mathcal{L}, \tag{1}$$

where $\mathbf{R}_{kl} \in \mathbb{C}^{M \times M}$ is the spatial correlation matrix, describing the correlation characteristics of the channel over the antenna array at the BS, and β_{kl} is the average channel gain determined by the large-scale fading terms. Note that the channel $\mathbf{h}_{kl}$ is independent for different (k, l) pairs. Since the location of the VUE changes in the order of seconds, the multipath components of the received signal can be considered unchanged over one block, which lasts several milliseconds [18]. Accordingly, in this work, $\beta_{kl}\mathbf{R}_{kl}$ is treated static in one block and assumed to be available[1].

The widely adopted block-fading channel model assumes that the channel is time-invariant in a coherence block consisting of T_c coherence time symbols and B_c coherence bandwidth symbols [1], [2]. Due to the movement of the VUEs, however, the actual channel will change over time.

---

[1]A small number of time-frequency resources is enough to estimate the spatial correlation matrix using existing methods such as the regularization approach [1, Sect. 3.3.3] and the staggered pilot-based method [19].

In this work, we focus on the temporal correlation of the channel coefficients in a transmission block. Following [11], the channel vector at the n-th symbol time, denoted using $\mathbf{h}_{kl}[n]$, is modeled as a function of its previous state $\mathbf{h}_{kl}[n-\tau]$ and an innovation component:

$$\mathbf{h}_{kl}[n] = \rho_{kl}[\tau]\mathbf{h}_{kl}[n-\tau] + \bar{\rho}_{kl}[\tau]\mathbf{z}_{kl}[n], \tag{2}$$

where $\rho_{kl}[\tau]$ is the channel normalized TCC with time lag $T_s\tau$ (T_s stands for the sampling period) computed according to

$$\rho_{kl}[\tau] \triangleq \frac{\mathbb{E}\{|\mathbf{h}_{kl}^{\mathrm{H}}[n-\tau]\mathbf{h}_{kl}[n]|\}}{\mathbb{E}\{\mathbf{h}_{kl}^{\mathrm{H}}[n]\mathbf{h}_{kl}[n]\}}, \tag{3}$$

$\bar{\rho}_{kl}[\tau] \triangleq \sqrt{1-\rho_{kl}^2[\tau]}$, and $\mathbf{z}_{kl}[n] \sim \mathcal{N}_\mathbb{C}(\mathbf{0}, \beta_{kl}\mathbf{R}_{kl})$ is the independent innovation component at instant n. Notice that $\rho_{kl}[\tau] \in [0,1]$, and the smaller $\rho_{kl}[\tau]$ is, the less correlated $\mathbf{h}_{kl}[n]$ and $\mathbf{h}_{kl}[n-\tau]$ are.

We then calculate $\rho_{kl}[\tau]$ for the more realistic non-isotropic scattering propagation scenario, in which the multipath components arrive from a limited AoA interval concentrated around a central direction. The von Mises distribution [20] is employed for AoA from VUE k to BS l: Denoting the AoA of a multipath component by θ, its PDF is given by

$$p_{kl}(\theta) = \frac{\exp\left[\kappa\cos\left(\theta-\theta_{kl}^p\right)\right]}{2\pi I_0(\kappa)}, \quad \theta \in [-\pi, \pi), \tag{4}$$

where $I_0(z) = \frac{1}{\pi}\int_0^\pi \cosh(z\cos\theta)d\theta$ stands for the zeroth-order modified Bessel function of the first kind [21, Eq. (9.6.16)], $\theta_{kl}^p \in [-\pi, \pi)$ is the central direction of the AoA interval, and the width is controlled by the factor $\kappa(\geqslant 0)$. According to [22], the normalized TCC is calculated by $\rho_{kl}[\tau] = \mathbb{E}_\theta\left[\exp\left(j2\pi f_k^m T_s\tau\cos\theta\right)\right]$, where $f_k^m = v_k f/c$ is the maximum Doppler shift with velocity v_k, and f and c represent the carrier frequency and the speed of light, respectively. Using $p_{kl}(\theta)$ in (4) and taking expectation with respect to θ, we have

$$\rho_{kl}[\tau] = \frac{I_0\left(\sqrt{\kappa^2 - (2\pi f_k^m T_s\tau)^2 + j4\pi\kappa\cos\left(\theta_{kl}^p\right)f_k^m T_s\tau}\right)}{I_0(\kappa)}. \tag{5}$$

In this work, we refer to (5) as the von Mises TCC model.

For the case of $\kappa = 0$, $\rho_{kl}[\tau] = J_0\left(2\pi f_k^m T_s\tau\right)$ is immediately obtained, where $J_0(z) = \frac{1}{\pi}\int_0^\pi \cos(z\cos\theta)d\theta$ is zeroth-order Bessel function of the first kind [21, Eq. (9.1.18)], and (5) reduces to the Jakes-Clarke TCC model based on the isotropic scattering assumption [6]. With a larger κ, the AoA interval becomes more concentrated. When κ is not too small, the width of the AoA interval is roughly equal to $2/\sqrt{\kappa}$ in radians [22]. For example, when $\kappa = 3$ and 10, the AoA interval widths are roughly 66° and 36°, respectively.

B. Uplink Channel Training

During the channel training phase, all VUEs transmit the pilot sequences, which are randomly assigned among them, to their serving BSs simultaneously. Recall that T symbols are reserved for this purpose. Assume that T mutually orthogonal

T-length pilot sequences $\{\boldsymbol{\varphi}_1,\ldots,\boldsymbol{\varphi}_T \in \mathbb{C}^T\}$, with $\|\boldsymbol{\varphi}_t\|^2 = T$, are adopted [23]. Moreover, $K > T$ is assumed, meaning that multiple VUEs will be assigned with a same pilot. Denote the index of the pilot assigned to VUE k to be $t(k)$, and $\mathcal{K}_{t(k)}$ as the set of VUEs that share $\boldsymbol{\varphi}_{t(k)}$. The interference between VUEs in $\mathcal{K}_{t(k)}$ causes the so-called pilot contamination [23].

Since T is usually a very small number ($T \ll D$), the channel is treated static during the training phase. The signal received over the T time instances by the serving BS of VUE k (assumed to be BS l) is given by

$$\mathbf{Y}_l^{\mathrm{p}} = \sqrt{p_k}\mathbf{h}_{kl}\boldsymbol{\varphi}_{t(k)}^{\mathrm{T}} + \sum_{i\in\mathcal{K}\backslash\{k\}}\sqrt{p_i}\mathbf{h}_{il}\boldsymbol{\varphi}_{t(i)}^{\mathrm{T}} + \mathbf{N}_l, \quad (6)$$

where $p_i (\geqslant 0)$ is the transmit power of VUE i, and $\mathbf{N}_l \in \mathbb{C}^{M \times T}$ is the noise matrix with i.i.d. elements $\sim \mathcal{N}_{\mathbb{C}}\left(0,\sigma^2\right)$.

In order to estimate $\mathbf{h}_{kl}$, BS l first cancels the interference from those VUEs assigned with orthogonal pilots by multiplying the $\mathbf{Y}_l^{\mathrm{p}}$ by the normalized conjugate of $\boldsymbol{\varphi}_{t(k)}$, which leads to the processed received pilot signal $\mathbf{y}_{t(k)l}^{\mathrm{p}} = \frac{1}{\sqrt{T}}\mathbf{Y}_l^{\mathrm{p}}\boldsymbol{\varphi}_{t(k)}^* \in \mathbb{C}^M$, given explicitly by

$$\mathbf{y}_{t(k)l}^{\mathrm{p}} = \sqrt{p_k T}\mathbf{h}_{kl} + \sum_{i\in\mathcal{K}_{t(k)}\backslash\{k\}}\sqrt{p_i T}\mathbf{h}_{il} + \mathbf{n}_{t(k)l}, \quad (7)$$

where $\mathbf{n}_{t(k)l} = \frac{1}{\sqrt{T}}\mathbf{N}_l\boldsymbol{\varphi}_{t(k)}^* \sim \mathcal{N}_{\mathbb{C}}\left(\mathbf{0},\sigma^2\mathbf{I}_M\right)$. The MMSE estimation of the channel vector is given by

$$\widehat{\mathbf{h}}_{kl} = \sqrt{p_k T}\beta_{kl}\mathbf{R}_{kl}\boldsymbol{\Psi}_{t(k)l}^{-1}\mathbf{y}_{t(k)l}^{\mathrm{p}} \quad (8)$$

with $\boldsymbol{\Psi}_{t(k)l} = \mathbb{E}\{\mathbf{y}_{t(k)l}^{\mathrm{p}}(\mathbf{y}_{t(k)l}^{\mathrm{p}})^{\mathrm{H}}\} = \sum_{i\in\mathcal{K}_{t(k)}}p_i T\beta_{il}\mathbf{R}_{il} + \sigma^2\mathbf{I}_M$. The estimation error $\widetilde{\mathbf{h}}_{kl} = \mathbf{h}_{kl}-\widehat{\mathbf{h}}_{kl}$ is uncorrelated with $\widehat{\mathbf{h}}_{kl}$. Moreover, let $\boldsymbol{\Phi}_{kl} = p_k T\beta_{kl}^2\mathbf{R}_{kl}\boldsymbol{\Psi}_{t(k)l}^{-1}\mathbf{R}_{kl}$, $\widehat{\mathbf{h}}_{kl} \sim \mathcal{N}_{\mathbb{C}}\left(\mathbf{0},\boldsymbol{\Phi}_{kl}\right)$ and $\widetilde{\mathbf{h}}_{kl} \sim \mathcal{N}_{\mathbb{C}}\left(\mathbf{0},\beta_{kl}\mathbf{R}_{kl} - \boldsymbol{\Phi}_{kl}\right)$.

C. Uplink Data Transmission

During the UL data transmission phase, the estimated channel $\widehat{\mathbf{h}}_{kl}$ given by (8) and the von Mises TCC model given by (5) are used to calculate the effective channel vectors. To be precise, $\widehat{\mathbf{h}}_{kl}$, which is obtained at the end of the training phase, is used for the initial channel vector $\mathbf{h}_{kl}[0]$, and the channel vector over which the n-th data symbol is transmitted, $n = 1,...,D$, is modeled as

$$\begin{aligned}\mathbf{h}_{kl}[n] &= \rho_{kl}[n]\mathbf{h}_{kl}[0] + \bar{\rho}_{kl}[n]\mathbf{z}_{kl}[n] \\ &= \rho_{kl}[n](\widehat{\mathbf{h}}_{kl}[0] + \widetilde{\mathbf{h}}_{kl}[0]) + \bar{\rho}_{kl}[n]\mathbf{z}_{kl}[n] \\ &= \rho_{kl}[n]\widehat{\mathbf{h}}_{kl}[0] + \tilde{\mathbf{e}}_{kl}[n], \end{aligned} \quad (9)$$

where $\tilde{\mathbf{e}}_{kl}[n] = \rho_{kl}[n]\widetilde{\mathbf{h}}_{kl}[0] + \bar{\rho}_{kl}[n]\mathbf{z}_{kl}[n]$, distributed following $\mathcal{N}_{\mathbb{C}}(\mathbf{0},\mathbf{E}_{kl})$ with $\mathbf{E}_{kl} = \beta_{kl}\mathbf{R}_{kl} - \rho_{kl}^2[n]\boldsymbol{\Phi}_{kl}$, is the accumulative error and is mutually independent of $\widehat{\mathbf{h}}_{kl}[0]$.

Since all VUEs transmit their data simultaneously, the received signal at BS l at symbol n, is given by

$$\mathbf{y}_l^{\mathrm{s}}[n] = \mathbf{h}_{kl}[n]x_k[n] + \sum_{i\in\mathcal{K}\backslash\{k\}}\mathbf{h}_{il}[n]x_i[n] + \mathbf{w}_l[n], \quad (10)$$

where $x_i[n] \sim \mathcal{N}_{\mathbb{C}}\left(0,p_i\right)$ is the signal transmitted from VUE i, and $\mathbf{w}_l[n] \sim \mathcal{N}_{\mathbb{C}}\left(\mathbf{0},\sigma^2\mathbf{I}_M\right)$ is the dependent noise. BS l

selects a receive combining vector $\mathbf{v}_{kl}[n] \in \mathbb{C}^M$ for VUE k, which is applied to the received signal $\mathbf{y}_l^{\mathrm{s}}[n]$ to obtain

$$\begin{aligned}\widehat{x}_k[n] &= \mathbf{v}_{kl}^{\mathrm{H}}[n]\mathbf{y}_l^{\mathrm{s}}[n] = \mathbf{v}_{kl}^{\mathrm{H}}[n]\mathbf{h}_{kl}[n]x_k[n] \\ &+ \sum_{i\in\mathcal{K}\backslash\{k\}}\mathbf{v}_{kl}^{\mathrm{H}}[n]\mathbf{h}_{il}[n]x_i[n] + \mathbf{v}_{kl}^{\mathrm{H}}[n]\mathbf{w}_l[n], \quad (11)\end{aligned}$$

and detects $x_k[n]$ from $\widehat{x}_k[n]$.

III. PERFORMANCE ANALYSIS

Based on the models developed in the previous section, we now analyze the UL transmission performance of the multi-cell massive MIMO network over the aging channels. The achievable user SE is adopted for performance evaluation.

Following the similar analysis methods as in [11], [12], and [23], the following result is derived.

Proposition 1. *In a multi-cell massive MIMO network, the achievable UL SE of VUE k over an aging channel (9) is given by*

$$\mathrm{SE}_k = \frac{1}{C}\sum_{n=1}^{D}\{\log_2\left(1 + \eta_k[n]\right)\}, \quad (12)$$

where $C = T + D$ and $\eta_k[n]$ is the instantaneous effective signal-to-interference-and-noise ratio (SINR) of the n-th data symbol, given by

$$\eta_k[n] = \frac{p_k\rho_{kl}^2[n]\left|\mathbf{v}_{kl}^{\mathrm{H}}[n]\widehat{\mathbf{h}}_{kl}[0]\right|^2}{\displaystyle\sum_{i\in\mathcal{K}\backslash\{k\}}p_i\rho_{il}^2[n]\left|\mathbf{v}_{kl}^{\mathrm{H}}[n]\widehat{\mathbf{h}}_{il}[0]\right|^2 + \mathbf{v}_{kl}^{\mathrm{H}}[n]\mathbf{Q}_{kl}\mathbf{v}_{kl}[n]} \quad (13)$$

with

$$\mathbf{Q}_{kl} = \sum_{i\in\mathcal{K}}p_i\mathbf{E}_{il} + \sigma^2\mathbf{I}_M. \quad (14)$$

Proof. Substituting (9) into (11), we obtain

$$\widehat{x}_k[n] = \underbrace{\rho_{kl}[n]\mathbf{v}_{kl}^{\mathrm{H}}[n]\widehat{\mathbf{h}}_{kl}[0]x_k[n]}_{\text{desired signal}} + \underbrace{\mathrm{IN}_k[n]}_{\text{interference plus noise}}, \quad (15)$$

where the interference plus noise term is given by

$$\begin{aligned}\mathrm{IN}_k[n] &= \sum_{i\in\mathcal{K}\backslash\{k\}}\rho_{il}[n]\mathbf{v}_{kl}^{\mathrm{H}}[n]\widehat{\mathbf{h}}_{il}[0]x_i[n] \\ &+ \sum_{i\in\mathcal{K}}\mathbf{v}_{kl}^{\mathrm{H}}[n]\tilde{\mathbf{e}}_{il}[n]x_i[n] + \mathbf{v}_{kl}^{\mathrm{H}}[n]\mathbf{w}_l[n]. \quad (16)\end{aligned}$$

The processed signal in (15) can be treated as a discrete memoryless interference channel with a random channel response $\mathbf{v}_{kl}^{\mathrm{H}}[n]\widehat{\mathbf{h}}_{kl}[0]$. After some algebraic operations, we calculate the desired signal power and the interference plus noise power and obtain (13). The details are omitted here to save space. $\square$

We would like to note that comparing to the existing works such as [6], [11], in which the channel TCC was assumed to be the same for all users, equation (13) gives us the flexibility to study channel aging in a wide range of scenarios. In particular, one can specify any heterogeneous AoA intervals for different users, which can be done, for example, according to the

standardized channel models or based on the actual positions and motions of the users in a network setting. We will adopt the latter approach in our simulations in Sect. IV. We would also like to note that by letting $\rho_{kl}[n] = 1$ for all k, l, and n, equation (13) reduces to the instantaneous SINR with the block-fading channel model that assumes no aging effect, and (12) also gives the achievable UL SE in this setting.

The maximum ratio (MR) combining scheme could be adopted at the BS, using the following combining vector:

$$\mathbf{v}_{kl}^{\text{MR}}[n] = \widehat{\mathbf{h}}_{kl}[0]. \tag{17}$$

MR combining maximizes the power of the desired signal but is prone to interference from signals from the non-orthogonal channels, which is the case in most practical situations. To maximize the instantaneous SINR, the BS can adopt the MMSE combining strategy. We note that the SINR in (13) has the form of a generalized Rayleigh quotient.

Corollary 1. *The SINR in (13) is maximized by the MMSE combining vector given in the following:*

$$\mathbf{v}_{kl}^{\text{MMSE}}[n] = p_k \left(\sum_{i \in \mathcal{K}} p_i \rho_{il}^2[n] \widehat{\mathbf{h}}_{il}[0] \widehat{\mathbf{h}}_{il}^{\text{H}}[0] + \mathbf{Q}_{kl} \right)^\dagger \widehat{\mathbf{h}}_{kl}[0]. \tag{18}$$

Proof. It follows from [23, Eq. (40)] since (18) minimizes the mean-squared error $\text{MSE} = \mathbb{E}\{|x_k[n] - \widehat{x}_k[n]|^2 | \{\widehat{\mathbf{h}}_{il}[0]\}\}$, which is the conditional MSE between the data signal $x_k[n]$ and the received signal $\widehat{x}_k[n]$ in (11) given the channel estimates. $\square$

We need to emphasize that owing to the TCC term, it is generally infeasible to derive (13) further into closed-form expressions. However, the SINRs can be easily computed using the Monte Carlo method for any given $\mathbf{v}_{kl}[n]$.

IV. NUMERICAL RESULTS AND DISCUSSION

A Manhattan grid scenario is set following 3GPP TR 36.885 [24] for the simulation, and a wrap-around is applied to mimic a large network deployment. In the center of each road grid, a BS employing a uniform linear array (ULA) is deployed, as shown in Fig. 1. VUEs are dropped on the lanes following a Poisson line process. Following [25], the average channel gain (in dB) is modeled as $\beta_{kl} = -34.53 - 38\log_{10}(d_{kl}) + X_{kl}$, where d_{kl} is the distance between antennas of VUE k and BS l, and $X_{kl} \sim \mathcal{N}(0, 10)$ is the lognormal shadow fading. The correlation matrix $\mathbf{R}_{kl}$ is calculated following the local scattering model [1, Sect. II], and the actual azimuth angle determined by the locations of a VUE is adopted for the central angle θ_{kl}^p of the AoA range, as shown in Fig. 1. The default parameter settings are given in Table I. The coherent bandwidth $B_c = 1/(2T_d)$ [13, Eq. (2.48)] is adopted, where T_d stands for the delay spread. In the simulations, $T_d = 5$ μs is chosen, which corresponds to 1.5 km path differences and leads to $B_c = 100$ kHz. The total number of symbols in a transmission block is given by $C = B_c T_{tb}$, where T_{tb} is the
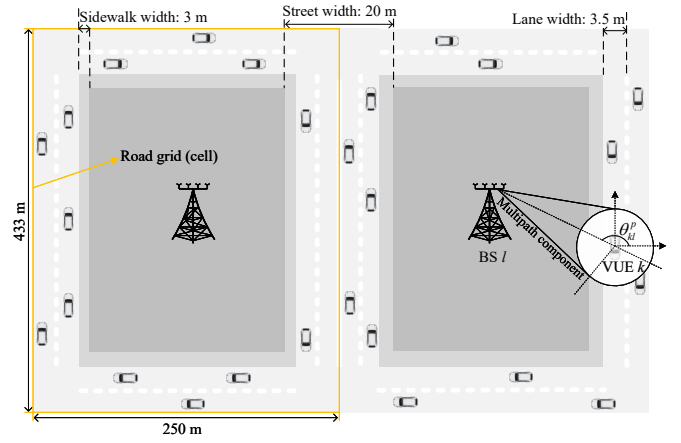

Fig. 1. Schematic diagram of the simulation scenarios with two cells.

Table I
SIMULATION PARAMETERS

Parameter	Value	Parameter	Value
Cell number L	16	Road grid size	250 m $\times$ 433 m
Sidewalk width	3 m	Street width	20 m
Lane width	3.5 m	VUE density	12 VUE/km/lane[1]
Power $p_k, k \in \mathcal{K}$[2]	0.1 W	VUE antenna height	1.5 m
Velocity $v_k, k \in \mathcal{K}$	60 km/h	BS antenna height	25 m
Antenna number M	100	Carrier frequency	2 GHz
Antenna spacing	0.075 m	Number of pilot T	20
Sampling period T_s	0.01 ms	Noise power density	-174 dBm/Hz

[1] The average inter-VUE gap in each lane is 2.5 sec $\times$ v [24, Table A.1.2-1], leading to an average number of 31 VUEs in each cell/grid.
[2] Means that all VUEs use the same value.

time duration of a transmission block. C will be called the transmission block size in this section.

The following area average SE metric (in bit/s/Hz) is adopted:

$$\text{ASE} = \sum_{k \in \mathcal{K}} \text{SE}_k / L, \tag{19}$$

which represents the average total SE obtained in each cell/grid in the simulated multi-cell scenario. If the channel does not age at all, one should make T_{tb} (or C) as large as possible. However, as the channel ages, the actual channel coefficient for data transmissions and the estimated channel coefficient becomes less and less correlated with time, resulting in a decline in the instantaneous SINR for the data symbols in a transmission block. When the channel ages to a certain extent, it becomes beneficial to perform channel training again at the cost of the T symbols. Accordingly, one may expect the existence of an optimal block length that maximizes the ASE performance.

In Fig. 2, the ASE curves are plotted against C under three settings: 1) a non-isotropic scattering scenario with $\kappa = 2.8$ for the von Mises TCC model, which equivalents a 68° AoA spread (see Sect. II-A and [25, Table 5.1] for the calculation); 2) the isotropic scattering scenario given by letting $\kappa = 0$, in which case, the von Mises TCC model reduces to the Jakes-Clarke TCC model; and 3) no channel aging, indicated using $\rho = 1$. Both MR and MMSE combining are evaluated. The re-
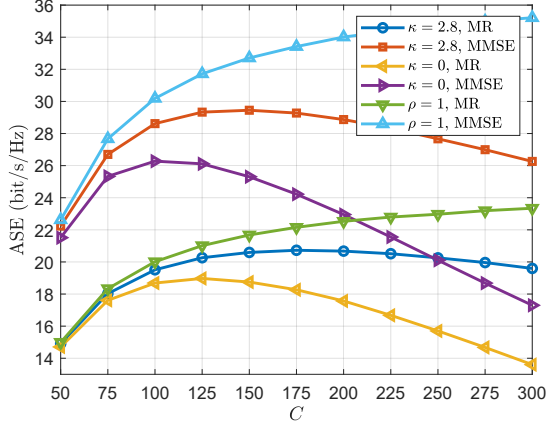
Fig. 2. The ASE performances of MR and MMSE combining with different choices of transmission block size C in different channel aging scenarios.

sults clearly show that the non-aging assumption overestimates the performance of massive MIMO greatly and leads to false ASE trends. When channel aging is considered, there exists an optimal choice C_{opt} for the transmission block size, which depends on both κ and the combining method adopted by the BS. In particular, with MMSE combining, ASE is maximized when $C \approx 150$ ($T_{tb} \approx 1.5$ ms) in the non-isotropic scattering setting ($\kappa = 2.8$), while in the isotropic scattering setting, the maximum ASE is achieved when $C \approx 100$ ($T_{tb} \approx 1$ ms). This means that if the Jakes-Clarke TCC model is misused for a non-isotropic scattering scenario, it will not only lead to an overly pessimistic performance prediction but also suggest a rather small transmission block, causing performance loss and unnecessarily high channel training cost eventually.

We also note that the channel TCC equals approximately to 0.8 at the end of a transmission block by setting $C = 300$ ($T_{tb} = 3$ ms) following the von Mises TCC model with $\kappa = 2.8$. The 20% decorrelation criterion is often adopted to determine the transmission block length, which, however, causes huge gaps as compared with the optimal ASE performances, as Fig. 2 clearly shows.

Fig. 3 presents the ASE heat maps for both MR and MMSE combining with channel aging for the range of $\kappa \in [0, 10]$ and $C \in [50, 400]$. The contour lines are also plotted. Note that the AoA spread increases from about $36°$ to $360°$ as κ decreases from 10 to 0. The following observations are made: Firstly, when fixing C to be a certain value, the absolute value of ASE achieved by MMSE combining degrades faster than that by MR combining, with the decreasing of κ. This means that although MMSE outperforms MR in all situations, the performance gain shrinks as κ gets smaller. Secondly, it is interesting to observe that C_{opt} is roughly given by a linear equation of κ for both MMSE and MR combining. In particular, the empirical equations under the simulation setting are $C_{\mathrm{MR,opt}}(\kappa) = 16.48\kappa + 113$ for MR and $C_{\mathrm{MMSE,opt}}(\kappa) = 13.29\kappa + 95$ for MMSE. They show that when MMSE combining is adopted, a smaller transmission block size optimizes the ASE performance, as compared with the MR combining. In scenarios with very small κ, however,
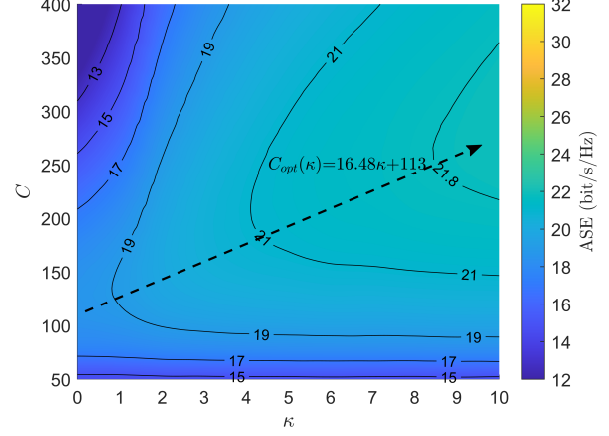
(a) MR combining
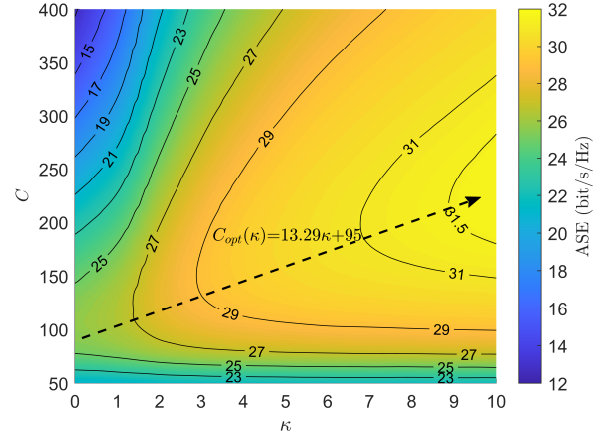
(b) MMSE combining

Fig. 3. The ASE heat map and contour lines as a function of κ and C.

$C_{\mathrm{MR,opt}}$ and $C_{\mathrm{MMSE,opt}}$ are closer.

In all the above simulations, the VUE velocity v (VUE subscript omitted) is set to be a same value for all VUEs, but it is also clear from (5) that channel aging is also affected by velocity through f_k^m. Therefore, considering the same setting as in Fig. 2, we show in Fig. 4 the simulated ASE results against v, with a fixed $C = 300$. The simulated results provide clear evidence that ASE will not change under the non-aging setting, but in aging scenarios, an increasing v will degrade the ASE performance. The results also show that the decrease in ASE is greater under the isotropic scattering scenario ($\kappa = 0$), and in addition, the decreasing rate is nonlinear with v. The nonlinearity can be seen most clearly with the isotropic scattering setting. We can thus infer that the choice of C_{opt} shall depend also on the average VUE velocity.

V. CONCLUSIONS AND FUTURE WORKS

In this paper, we have studied the impact of channel aging on UL SE performance in a multi-cell massive MIMO vehicular network in non-isotropic scattering scenarios. The von Mises distribution has been adopted for AoA modeling, which leads to a tunable channel TCC model adjusted by a parameter κ, and allows for finer-grained studies within and
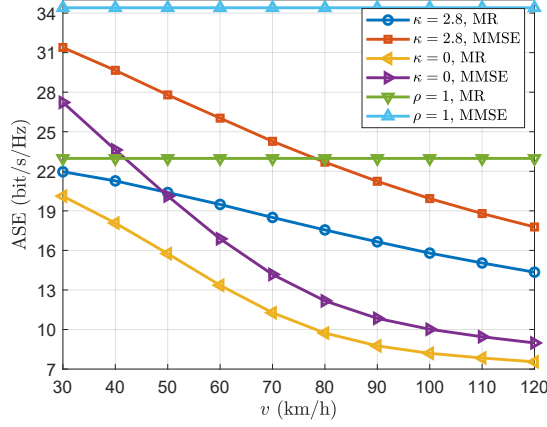
Fig. 4. The ASE performances of MR and MMSE combining with different VUE velocities v in different channel aging scenarios.

between different AoA spread conditions. We have focused on the impact of transmission block size C and VUE velocity v on the area mean SE metric under different κ conditions. The simulated results in a Manhattan grid scenario have shown that under different AoA spread conditions, there are different optimal choices for C, which depends also on the combining strategies adopted at the BSs and the VUEs' velocity. In particular, when the velocity level is fixed, C_{opt} is empirically given by two linear equations of κ for MMSE and MR combining. The results emphasize the importance of accurate channel aging models that fit the actual scattering conditions in providing correct guidance to the design and operation of massive MIMO systems.

Owing to space limitation, we leave the optimal design of C considering both κ and v to future work. We also leave other related issues to future work, such as spatial correlation, pilot overhead, power allocation, etc. The impact of channel aging on the downlink and the influence of a heterogeneous non-isotropic scattering environment will be further investigated.

REFERENCES

[1] E. Björnson, J. Hoydis, and L. Sanguinetti, "Massive MIMO networks: Spectral, energy, and hardware efficiency," *Found. Trends Signal Process.*, vol. 11, no. 3-4, pp. 154–655, 2017.

[2] T. L. Marzetta, E. G. Larsson, H. Yang, and H. Q. Ngo, *Fundamentals of massive MIMO*. Cambridge, U.K.: Cambridge Univ. Press, 2016.

[3] L. Ding, Y. Wang, P. Wu, L. Li, and J. Zhang, "Kinematic information aided user-centric 5G vehicular networks in support of cooperative perception for automated driving," *IEEE Access*, vol. 7, pp. 40 195–40 209, 2019.

[4] Z. MacHardy, A. Khan, K. Obana, and S. Iwashina, "V2X access technologies: Regulation, research, and remaining challenges," *IEEE Commun. Surveys Tuts.*, vol. 20, no. 3, pp. 1858–1877, 2018.

[5] Y. Ge, W. Zhang, F. Gao, S. Zhang, and X. Ma, "High-mobility massive MIMO with beamforming network optimization: Doppler spread analysis and scaling law," *IEEE J. Sel. Areas Commun.*, vol. 38, no. 12, pp. 2889–2902, 2020.

[6] K. T. Truong and R. W. Heath, "Effects of channel aging in massive MIMO systems," *J. Commun. Netw.*, vol. 15, no. 4, pp. 338–351, 2013.

[7] H. Yin, H. Wang, Y. Liu, and D. Gesbert, "Addressing the curse of mobility in massive MIMO with prony-based angular-delay domain channel predictions," *IEEE J. Sel. Areas Commun.*, vol. 38, no. 12, pp. 2903–2917, 2020.

[8] C. Kong, C. Zhong, A. K. Papazafeiropoulos, and M. Matthaiou, "Sum-rate and power scaling of massive MIMO systems with channel aging," *IEEE Trans. Commun.*, vol. 63, no. 12, pp. 4879–4893, 2015.

[9] A. K. Papazafeiropoulos, "Impact of general channel aging conditions on the downlink performance of massive MIMO," *IEEE Trans. Veh. Technol.*, vol. 66, no. 2, pp. 1428–1442, 2016.

[10] R. Chopra, C. R. Murthy, and H. A. Suraweera, "On the throughput of large MIMO beamforming systems with channel aging," *IEEE Signal Process. Lett.*, vol. 23, no. 11, pp. 1523–1527, 2016.

[11] R. Chopra, C. R. Murthy, H. A. Suraweera, and E. G. Larsson, "Performance analysis of FDD massive MIMO systems under channel aging," *IEEE Trans. Wireless Commun.*, vol. 17, no. 2, pp. 1094–1108, 2017.

[12] J. Zheng, J. Zhang, E. Björnson, and B. Ai, "Impact of channel aging on cell-free massive MIMO over spatially correlated channels," *IEEE Trans. Wireless Commun.*, 2021, to appear.

[13] D. Tse and P. Viswanath, *Fundamentals of wireless communication*. Cambridge, U.K.: Cambridge Univ. Press, 2005.

[14] Q. Zhu, Y. Yang, C. Wang, Y. Tan, J. Sun *et al.*, "Spatial correlations of a 3-D non-stationary MIMO channel model with 3-D antenna arrays and 3-D arbitrary trajectories," *IEEE Wireless Commun. Lett.*, vol. 8, no. 2, pp. 512–515, 2018.

[15] S. Wang, A. Abdi, J. Salo, H. M. El-Sallabi, J. W. Wallace *et al.*, "Time-varying MIMO channels: Parametric statistical modeling and experimental results," *IEEE Trans. Vehi. Technol.*, vol. 56, no. 4, pp. 1949–1963, 2007.

[16] X. Cheng, Q. Yao, C. Wang, B. Ai, G. L. Stuber *et al.*, "An improved parameter computation method for a MIMO V2V rayleigh fading channel simulator under non-isotropic scattering environments," *IEEE Commun. Lett.*, vol. 17, no. 2, pp. 265–268, 2013.

[17] A. F. Molisch, *Wireless communications*, 2nd ed. New Jersey, NJ, USA: John Wiley & Sons Inc., 2012.

[18] X. Xia, K. Xu, S. Zhao, and Y. Wang, "Learning the time-varying massive MIMO channels: Robust estimation and data-aided prediction," *IEEE Trans. Veh. Technol.*, vol. 69, no. 8, pp. 8080–8096, 2020.

[19] K. Upadhya and S. A. Vorobyov, "Covariance matrix estimation for massive MIMO," *IEEE Signal Process. Lett.*, vol. 25, no. 4, pp. 546–550, 2018.

[20] Q.-U.-A. Nadeem, A. Kammoun, M. Debbah, and M.-S. Alouini, "A generalized spatial correlation model for 3D MIMO channels based on the fourier coefficients of power spectrums," *IEEE Trans. Signal Process.*, vol. 63, no. 14, pp. 3671–3686, 2015.

[21] M. Abramowitz and I. A. Stegun, *Handbook of mathematical functions with formulas, graphs, and mathematical tables*, 9th ed. New York, NY, USA: US Government printing office, 1964, vol. 55.

[22] A. Abdi, J. A. Barger, and M. Kaveh, "A parametric model for the distribution of the angle of arrival and the associated correlation function and power spectrum at the mobile station," *IEEE Trans. Veh. Technol.*, vol. 51, no. 3, pp. 425–434, 2002.

[23] L. Sanguinetti, E. Björnson, and J. Hoydis, "Toward massive MIMO 2.0: Understanding spatial correlation, interference suppression, and pilot contamination," *IEEE Trans. Commun.*, vol. 68, no. 1, pp. 232–257, 2019.

[24] 3GPP, "3rd generation partnership project; technical specification group radio access network; study on lte-based V2X services; (Release 14)." Tech. Rep. 36.885 V14.0.0, June. 2016.

[25] ——, "3rd generation partnership project; technical specification group radio access network; spatial channel model for multiple input multiple output (MIMO) simulations (Release 16)." Tech. Rep. 25.996 V16.0.0, July. 2020.